VERSITA

Acta Geophysica
vol. 61, no. 2, Apr. 2013, pp. 422-444
DOI: 10.2478/s11600-012-0071-3

Geoelectrical and Hydrochemical Investigations for Characterizing the Salt Water Intrusion in the Khanasser Valley, Northern Syria

Jamal ASFAHANI and Boulos ABOU ZAKHEM

Geology Department, Atomic Energy Commission, Damascus, Syria
e-mail: csientific@aec.org.sy

Abstract

An integrated approach of geoelectrical and hydrochemical investigation surveys was proposed for indicating contact regions between saline and fresh groundwater in the Khanasser valley region, northern Syria. The qualitative and quantitative interpretations of 34 vertical electrical soundings (VES) enable to characterize the salt water intrusion laterally and vertically. The established iso-apparent resistivity maps for different AB/2 spacings obviously indicate the presence of a low-resistivity (less than 4 Ohm·m) zone related to the salt water intrusion in the Quaternary and Paleogene deposits. The different hydrochemical and geophysical parameters, such as electrical resistivity, total dissolved solids (TDS) and major ions concentrations used to characterize the salt water intrusion gave almost similar results in locating and mapping the different boundaries of the groundwater salinity. The proposed approach is useful for mapping the interface between different groundwater qualities, and can be therefore used to successfully characterize the salt water intrusion phenomenon in other semi-arid regions. The application of such an approach is a powerful tool and can be used for water resource management in the water scarce areas.

Key words: groundwater, electrical resistivity, salt water intrusion, Khanasser valley, Syria.

1. INTRODUCTION

The study area is situated in the Khanasser valley, which is one of the integrated research sites of International Center for Agricultural Research in the Dry Areas (ICARDA) National Resource Management Program. In fact, the objective of choosing this site is to address problems related to the marginal dry land environments. The diversity and dynamics of the natural resources and livelihoods, poverty, and the relatively easy accessibility make Khanasser a prime candidate. This research is carried out in collaboration between three scientific institutions: Syrian Atomic Energy Commission (AECS), ICARDA, and Bonn University, Germany. The scientific program includes regular monitoring of groundwater levels and water chemistry, water use assessment, recharge studies, pumping tests, and geophysical surveys, aimed at determining potential groundwater use and providing information for defining sustainable resource management strategies.

The valley is located in northern Syria, approximately 70 km southeast of the city of Aleppo, and directly south of the Jaboul salt lake. The area is semi-arid and is located at the fringe of the Syrian steppe (Hoogeveen and Zobisch 1999). The annual rainfall of the area is 200-250 mm, with high annual and inter-annual variability (Soumi 1991). The total surface of the study area is 322.5 km^2. The valley lies 300-400 m a.s.l., between the hills of Jebel Shbith in the east and Jebel Al Hass in the west (Figs. 1 and 2). The Khanasser valley is oriented in the north-south direction. A gently undulating plain with a shallow network of wide dry erosion channels characterizes the valley. The hills of Jebel Al Hass and Jebel Shbith form gently rolling plateaus, which end in well-defined steep scarps towards the valley with V-shaped erosion channels.

Hydrologically, the Khanasser valley is situated on the border between two surface water catchments. The northern part of the area belongs to the Jaboul catchment and the drainage pattern is directed towards the Jaboul salt lake (sabkha). The hydraulic head changes from 318 m a.s.l. near Hawwaz to less than 310 m a.s.l. in the vicinity of Jaboul salt lake, which corresponds to about 0.001 as a hydraulic gradient. The southern part belongs to the steppe catchment and surface water drains towards a salt depression (sabkha) in the south. The water dividing line between the two basins lies in the vicinity of the line between Al Hobs and Serdah villages (Hoogeveen and Zobisch 1999, Asfahani 2007a). The study area of the present paper is located at the north of this water dividing line (Fig. 1).

The scarcity and the salinity of water resources increase from south to north and represent a serious obstacle in the development of the region.

The role of surface geophysical methods in hydrology domain for evaluating the groundwater resources is very well known, and several papers have

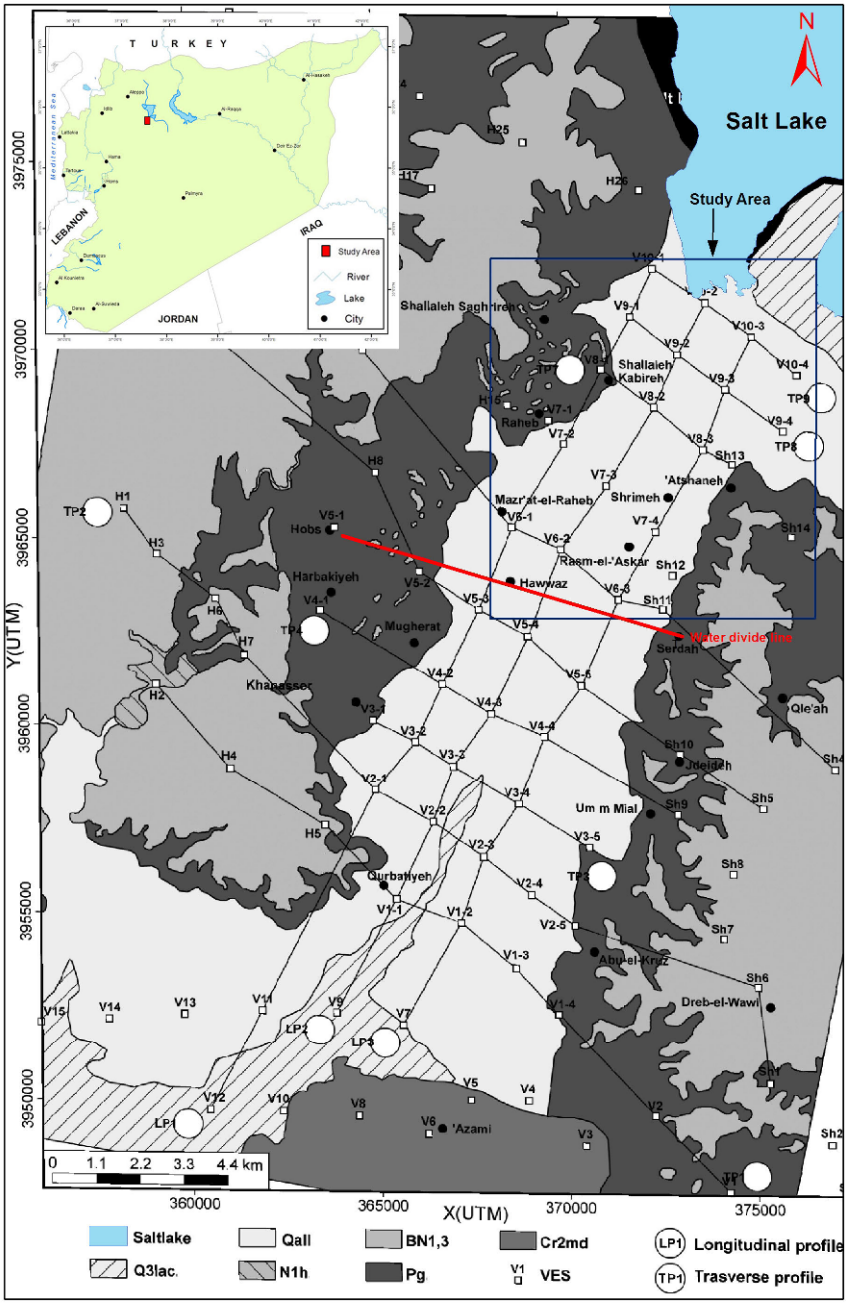

Fig. 1. Geological map of the Khanasser valley (after Ponikarov1964), the locations of vertical electrical soundings (VES) and study area. Colour version of this figure is available in electronic edition only.

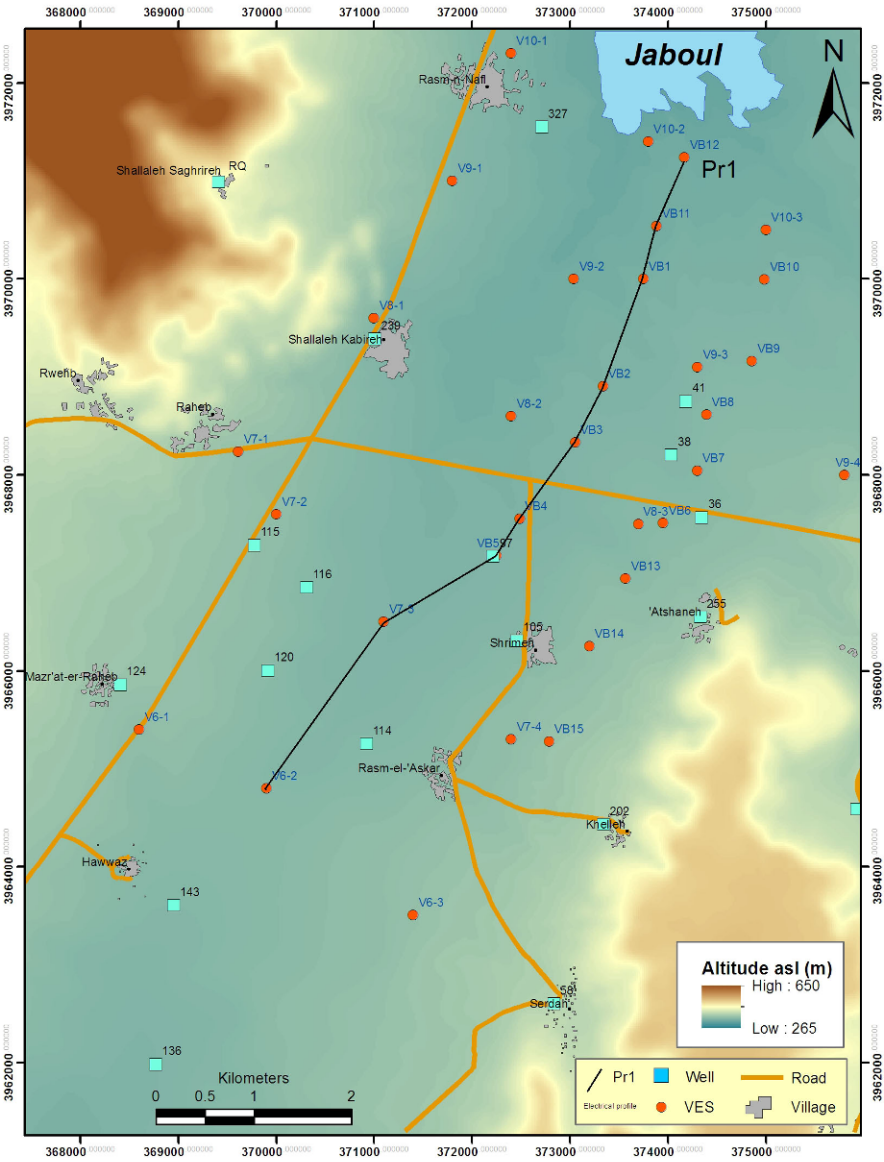

Fig. 2. Hillshaded digital elevation model ilustrating the relief of the study area, Khanasser valley, vertical electrical sounding (VES), and sampling wells location. Colour version of this figure is available in electronic edition only.

been published in this regards (Reilly and Goodman 1985, Ayers 1989, Hoekstra 1990, Asfahani 2007a, b, c). In addition, an integration of both geoelectrical and hydrochemical methods have been already applied for

groundwater quality investigation (Todd 1980, Hussein and Awad 2006, Al-Sayed and El-Qady 2007).

Groundwater investigations, particularly in semi-arid regions, are becoming a worldwide concern due the need of sustainable water resources. The geoelectrical methods may widely contribute in this regards for being inexpensive, and because they can be easily carried out in a reasonable time.

The application of geoelectrical surveying for delineating salt-water intrusion has been reported in the literature (*e.g.*, Nassir and Lee 1998, Samsudin *et al*. 1997, Loke 1996).

The present research mainly focuses on the application of the geoelectrical and hydrochemical investigations in order to characterize the saline water intrusion in the northern part of the Khanasser valley. The joint use of both hydrochemical (total dissolved solids, TDS, and the major ions concentrations) and geoelectrical methods is applied for mapping the boundary between fresh, brackish, and saline groundwater.

2. GEOLOGICAL SETTING

A geological map of the valley is shown in Fig. 1 (Ponikarov 1964). The oldest formation in the area is the Maestrichtian, described as a water-confining layer of 150-200 m thickness (Ponikarov 1964). This formation outcrops in the southern part of the valley, and consists of marl, clay, clayey limestone with flint intercalations, and phosphate interbeds.

The Paleogene formation is situated on the top of the Maestrichtian, with a maximum thickness exceeding 220 m. It comprises lower Eocene and Middle Eocene formations, consisting of clayey, chalky limestone, and silicified limestone (Ponikarov 1964). Both the middle and the lower Eocene contain localized aquifers with low productivity (ACSAD 1984).

Upper Miocene basalts are located on top of the Paleogene rock and found in the west on Jebel Al Hass, and in the east on Jebel Shbith. The average thickness of this basalt layer is 10 m, with a maximum exceeding 40 m. These formations do not contain groundwater resources in the valley.

A thick Quaternary deposit of more than 25 m is present in the center of the valley, and consists in proluvial, alluvial, and lacustrine deposits. Gypsum can be found in the lacustrine deposits. This formation contains unconfined groundwater in conglomerate-breccia and in some sand deposits.

3. PREVIOUS GEOPHYSICAL RESEARCHES

Electrical resistivity surveys are usually designed to measure the electrical resistivity of subsurface material. Vertical electrical soundings (VES) surveying with Schlumberger configuration were applied to conduct those electrical surveys in the study area. In such a configuration, the potential electrodes (M and N) remain fixed and the current electrodes (A and B) are

symmetrically expanded about the center of the spread. For a given position of the potential and current electrodes, the apparent resistivity, ρa, is expressed by the following equation:

$$\rho a = \frac{2\pi}{\frac{1}{AM} - \frac{1}{BM} - \frac{1}{AN} + \frac{1}{BN}} \frac{\Delta V}{I},$$

where I is the current introduced into the Earth, ΔV is the potential difference between the potential electrodes, and AM, BN, AN, and BN are interelectrodic spacings.

Ninety-six VES were carried out during this project (Asfahani 2007a, 2011). The location of those VES is shown in Fig. 1. A minimum current electrode spacing AB = 6 m (AB/2 = 3) and maximum AB = 1000 m (AB/2 = 500 m) were used for all of them.

The best-fit inversion of the 96 VES, distributed on the 12 transverse and longitudinal profiles, enabled identifying the subsurface geometry of the valley and the geoelectrical characteristics of the Quaternary, Paleogene, and Maistrechtian deposits (Asfahani 2007a). Asfahani (2007a, 2012b) also focused on the presence of two main geological structures, one in the north and the other in the south. The line joining Hobs and Serdah clearly separates those two structures. This remark was confirmed for all the geoelectrical maps corresponding to different spacings AB/2 (from 3 to 500 m), inferring that a clear deep tectonic feature is present along this joining line.

The boundaries of paleosabkhas related to Quaternary and Paleogene were also delineated (Asfahani 2007a).

Asfahani and Radwan (2007) proposed a tectonic evolutionary scenario for the valley and determined its hydrogeological characteristics, depending on both the results of traditional VES interpretation and the results of enhanced method of Pichgin and Habibullaev (1985). An approach for groundwater exploration in areas of prominent relief and topography in dry areas, such as Khanasser valley, was consequently established and its validity was also estimated.

Asfahani (2007b, 2011) related the earth resistivity, ρe, resulting from VES interpretation (carried out near the existing wells) with known measured groundwater TDS values of water samplings taken from the existing wells at several known depths. The TDS salinity variation correlated with earth resistivity was investigated both in lateral and vertical directions for different current electrode spacing AB/2. The spatial distribution of fresh, brackish, and salt water zones and its variation along the longitudinal profiles LP1, LP2, and LP3 were established through converting resistivity interpretative model into different groundwater quality areas (Asfahani 2007b, 2011). An alternative approach based on the use of VES survey has

been recently described for the determination of Quaternary transmissivity (Asfahani 2012a).

4. GEOPHYSICAL AND HYDROCHEMICAL INVESTIGATIONS

The salt water intrusion in the northern part of the Khanasser valley has been characterized by an integration of geophysical and hydrochemical investigations, summarized as follows:

- The geophysical surveying encompassed a total of 34 VES.
- The hydrochemical investigation consisted of analysis of shallow groundwater samples collected from 16 monitoring wells (KV) in two different campaigns (May and November 2001). Electrical conductivity (EC), pH, temperature, and total alkalinity (HCO_3^-) were measured *in situ*, while major elements were determined in the laboratory of the Atomic Energy Commission (AEC) by using the Ion Chromatograph (Dionex 120).
- The location of the VES and the monitoring wells are shown in Fig. 2.

5. RESULTS AND DISCUSSION

The Khanasser valley has been geophysically characterized as a whole with its regional surroundings by Asfahani (2007a, b, 2011), and Asfahani and Radwan (2007). The present research mainly focuses on the study of the salt water intrusion in the northern sector (Fig. 2). To this aim, additional VES were carried out (termed locally VB) in order to characterize as well as possible the salt water intrusion phenomenon (Fig. 2).

It is to mention that electrical resistivity signature of each geological formation has been calibrated and identified through carrying out resistivity measurements on the outcrops of those formations (Quaternary, Paleogene, and Maestrichtian), for which the resistivity response of the stratigraphic formation is known (Asfahani 2007a). It is therefore justified to relate the lateral and vertical resistivity variations to the salinity variations.

Figure 3 shows two typical examples of measured and fitted apparent resistivity curves collected in locations VB2 and VB5, and their equivalent best-fit inverted models (theoretical models), with rms error of 1.7 and 2.2%, respectively. The theoretical model includes the real resistivities and thicknesses of the final inverted geoelectrical model.

Iso-apparent resistivity maps have been constructed for different espacings AB/2, in order to study the lateral variations of the apparent resistivity at several penetration depths. Figures 4 and 5 show two examples of those maps for AB/2 = 70 and 100 m, which indicate the presence of a N-36 East elongated-shaped low-resistive zone (< 4 Ohm·m), interpreted as the geoelectrical response to a saline groundwater intrusion affecting the Qua-

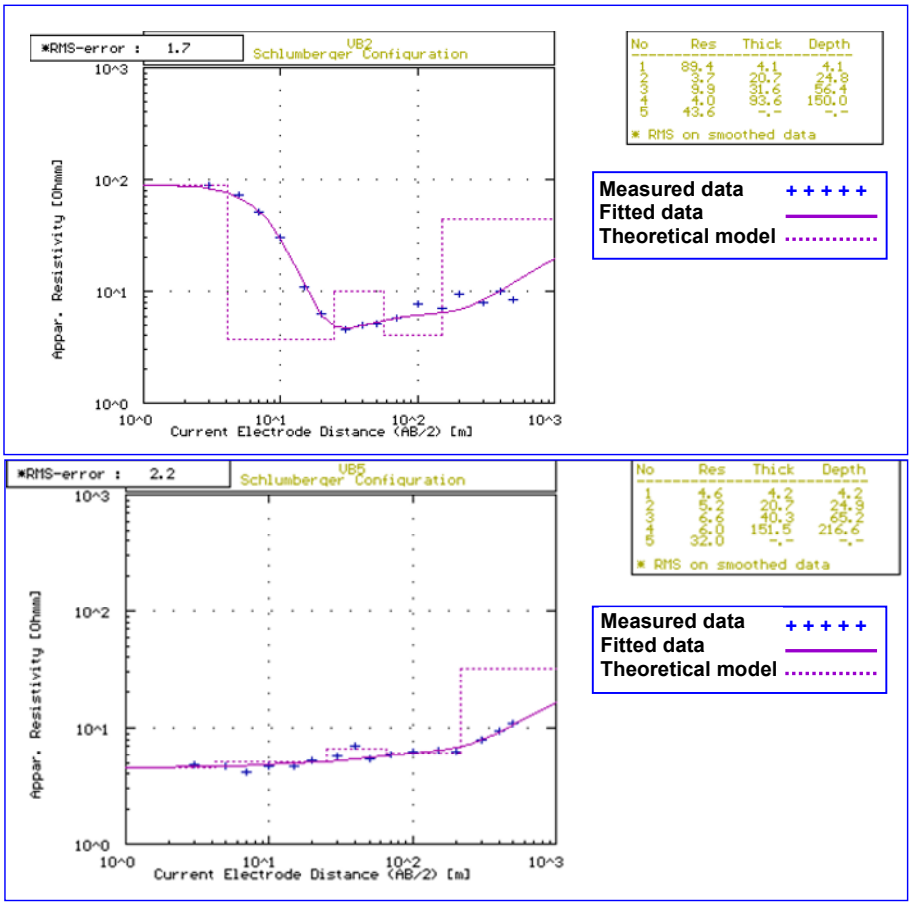

Fig. 3. Two VES examples of electrical field curves in VB2 and VB5 and their inverted 1D-models.

ternary and Paleogene deposits. It is to note that the Surfer-9 program is used for drawing those maps by using the geostatistical flexible Kriging method for the data gridding with a spacing of 75 pixel size.

Figure 6 shows the variation of electrical resistivity for different penetration depths of AB/2 of 40, 50, 70, 100, 150, and 200 m. The low-resistivity zone and its variation with depth are well distinguished for those AB/2, where the width of this zone increases with increasing AB/2. The chemical composition of shallow Quaternary groundwater is shown in Table 1.

The measured EC in the Jaboul salt lake (SL), which is used for salt exploitation when it becomes completely dry in the summer, ranges between 50 and 130 mS/cm. The measured EC is low in the recharge zone in Al Hass

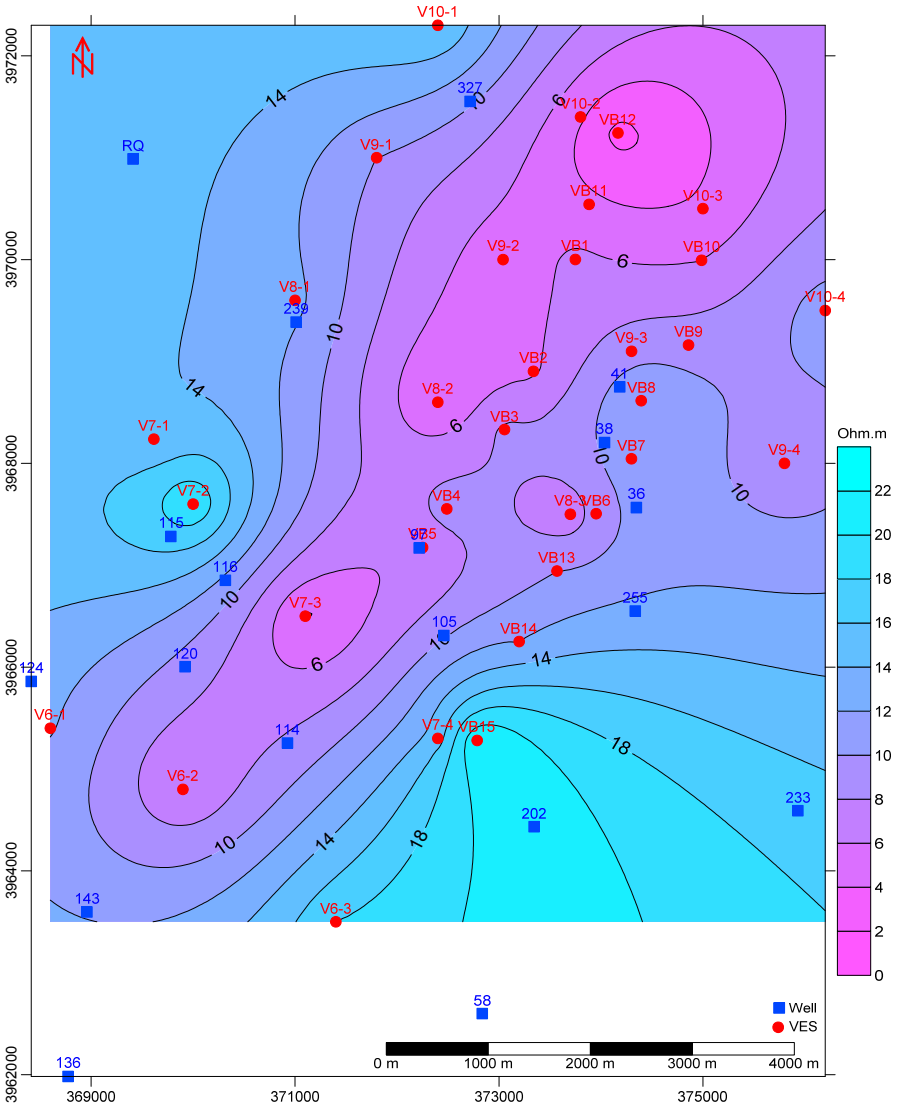

Fig. 4. Iso-apparent resistivity map for AB/2 = 70 m. Colour version of this figure is available in electronic edition only.

and Shbeith mountains, and is generally less than 2 mS/cm in both Roman canal (RQ, termed locally as Qanat) and well No. 202, as shown on the EC distribution map for shallow waters (Fig. 7). The EC increases from the borders to the axe of the valley paralleled to the groundwater flow path (from recharge areas to the valley axe). The EC reaches 8 mS/cm in the valley axe, where the water is used for irrigation and drinking cattle (wells Nos. 115,

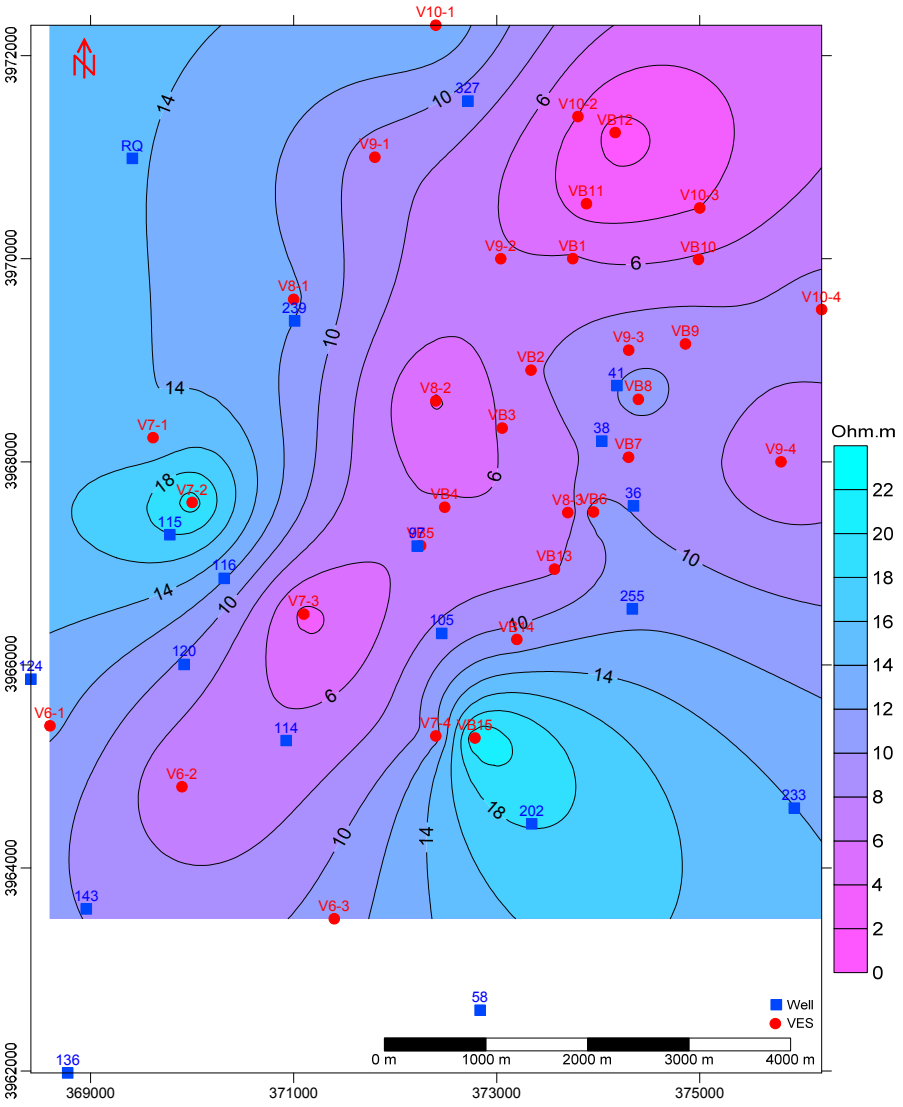

Fig. 5. Iso-apparent resistivity map for AB/2 = 100 m. Colour version of this figure is available in electronic edition only.

116, 120, 124, 239, 202, 36, and 255). It dramatically increases in some areas corresponding to the Quaternary deposits in northern part of the valley near the sabkha salt lake, where it ranges between 8 and 10 mS/cm (wells Nos. 38, 41 114, 136, and 143) and reaches its maximum of 25 mS/cm in well 97. Such an increase in the EC is due to the salt water intrusion into the fresh-brackish shallow groundwater, where an up-coning of salt water is

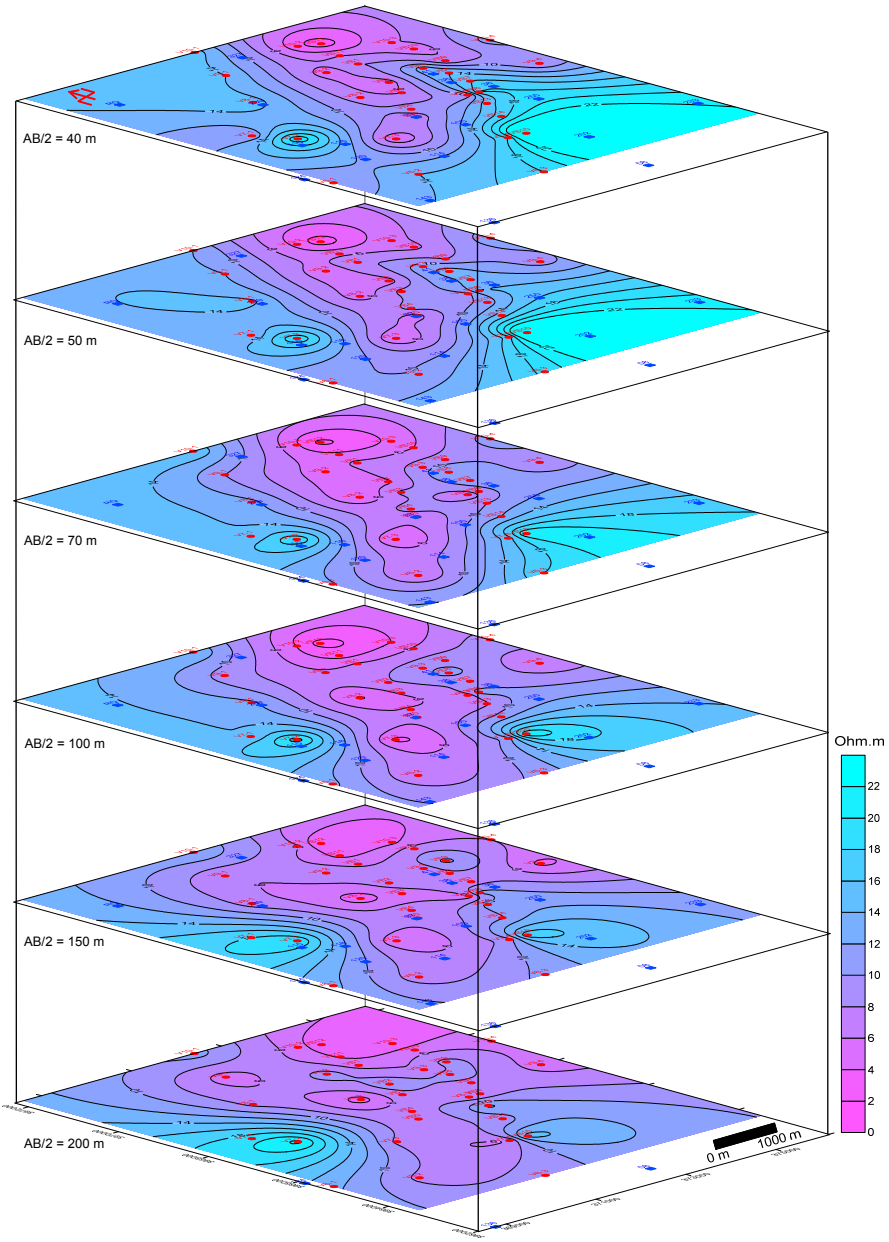

Fig. 6. Bloc diagram of iso-apparent resistivity maps for AB/2 of 40, 50, 70, 100, 150, and 200 m. Colour version of this figure is available in electronic edition only.

possible in well 97 location, due to the over exploitation of groundwater. It should be highlighted that the EC-anomaly (high value) is concentrated

Table 1

Chemical composition of shallow Quaternary groundwater in Khanasser valley, 5/2001

Code KV	EC [mS/cm]	*T* [°C]	pH	Ca^{++} [mg/l]	Mg^{++} [mg/l]	$Na^{+}+K^{+}$ [mg/l]	SO_4^{-} [mg/l]	Cl^{-} [mg/l]	HCO_3^{-} [mg/l]	NO_3^{-} [mg/l]	TDS [mg/l]	MR* [%]
SL	57.30	16	9.8	961.0	928.4	14799.8	9360.0	18503.8	183.5	31.8	44768	100.0
RQ	0.95	19	8.8	65.2	16.9	65.1	120.0	105.7	118.8	25.8	518	0.0
36	2.88	22	8.1	192.9	106.6	278.6	618.8	407.4	87.2	116.8	1808	1.6
38	7.73	21	7.8	502.1	297.9	854.3	1751.6	1339.0	90.3	152.9	4988	6.7
41	8.06	18	7.8	572.2	613.1	1905.7	3832.8	2851.1	82.4	182	10039	14.9
58	3.99	23	7.9	270.2	143.3	373.2	950.0	574.2	125.1	130.7	2567	2.5
97	26.54	21	7.9	1023.3	605.5	3691.6	4795.9	4920.0	85.4	251.8	15374	26.2
105	4.89	21	7.9	457.0	161.7	464.6	1419.5	670.8	90.0	139.4	3403	3.1
114	9.99	21	7.8	455.2	313.1	1258.7	1669.3	1979.9	106.8	176.4	5959	10.2
115	2.31	21	8.1	122.6	51.6	282.4	418.5	340.5	170.8	46.0	1432	1.3
116	3.30	23	8.0	160.2	81.9	436.9	565.8	573.3	106.8	66.9	1992	2.5
120	5.24	21	7.9	264.0	134.0	792.9	958.6	1070.4	90.9	111.4	3422	5.2
124	3.30	22	8.0	222.3	91.3	366.0	862.9	352.9	85.4	115.7	2097	1.3
136	8.14	21	8.0	650.2	236.7	887.9	1753.1	1548.6	114.4	130.5	5321	7.8
143	10.36	24	7.7	957.2	412.9	1626.9	2102.6	3188.5	126.6	145.6	8560	16.8
202	1.26	23	8.0	90.6	36.9	77.3	155.5	120.4	128.1	75.5	684	0.1
233	2.60	23	7.6	291.4	173.2	698.9	1238.6	917.6	151.3	130.2	3601	4.4
239	3.28	22	7.9	140.8	77.7	407.2	494.2	621.9	158.0	111.5	2011	2.8
255	2.21	25	7.9	118.0	59.9	205.2	271.9	316.6	144.6	12.4	1129	1.1
327	3.16	21	7.6	161.7	95.3	362.5	553.6	542.7	176.9	112.9	2006	2.4

Explanations: SL – Jaboul salt lake, RQ – Roman canal, 36 – Well number.
*estimated Mixing Ratios (MR) % (fraction of salt water within groundwater).

around the well 97, where there is a significant difference between both EC and electrical resistivity distribution patterns (Figs. 4, 5, and 7). This punctual difference between the EC and the electrical distributions is justified by an interpolation artifact due to the irregular space-distribution of the observation wells, with poor coverage in the valley axe, especially at the Jaboul salt lake neiborhood (Fig. 2). A more accurate assessement of the salt water intrusion into the valley is obtained by a regular and extensive grid of VES, as thus performed, allowing to investigate the salinity distribution in areas where no observation wells exist. This example of difference between the salinity patterns assessed by punctual EC water sampling records and extensive VES surveying proves the capability of the geoelectrical methods as a useful tool that may improving meaningfully the investigation of a salt water intrusion.

The intrusion phenomenon observed in the northern part of the Khanasser valley has been characterized through the study of the profile

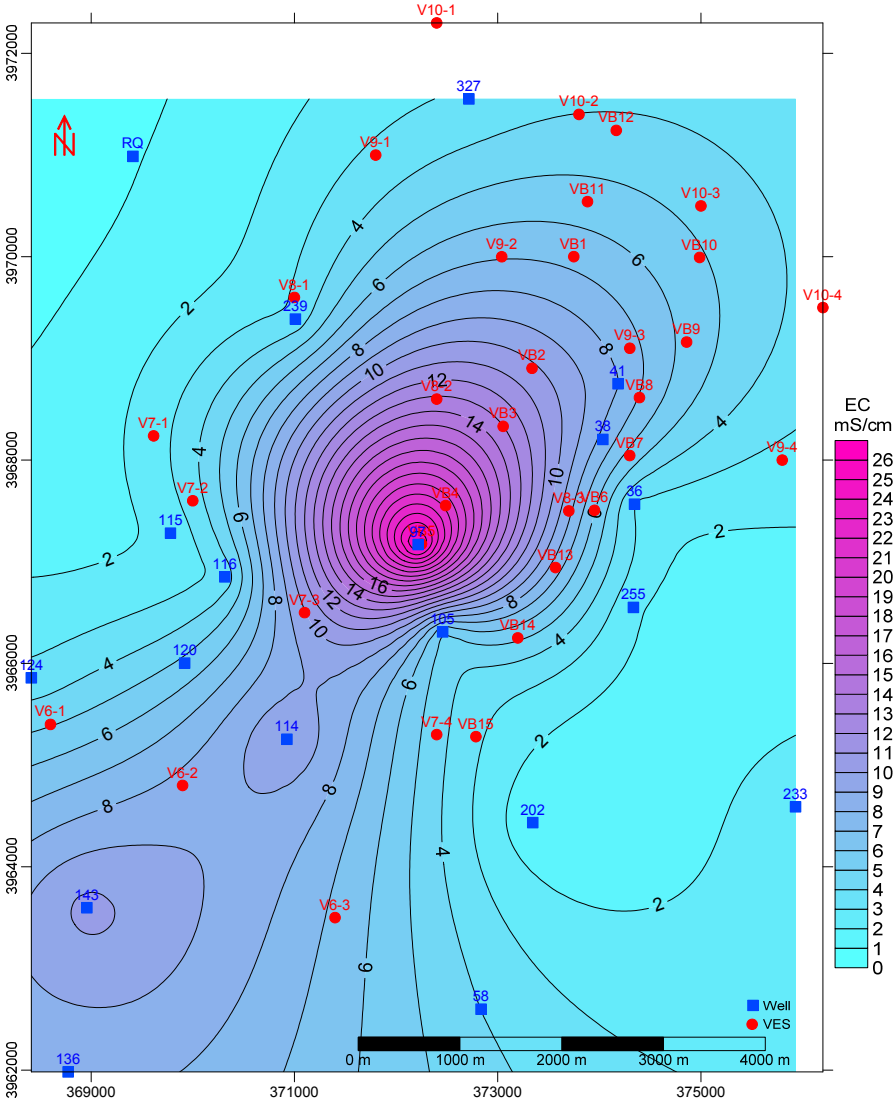

Fig. 7. Electrical conductivity distribution (EC) for shallow groundwater (Quaternary aquifer). Colour version of this figure is available in electronic edition only.

(Pr-1) of NE-SW direction and 8.67 km long. The raw resistivity of nine VES data distributed along Pr–1 have been interpreted by using RES2DINV program, in order to obtain a 2D inverted resistivity model. Figure 8a shows the inverted model with rms of 4.9%, obtained after 5 iterations, where a real penetration depth of 80 m is reached for AB/2 from 3 to 200 m. Figure 8b

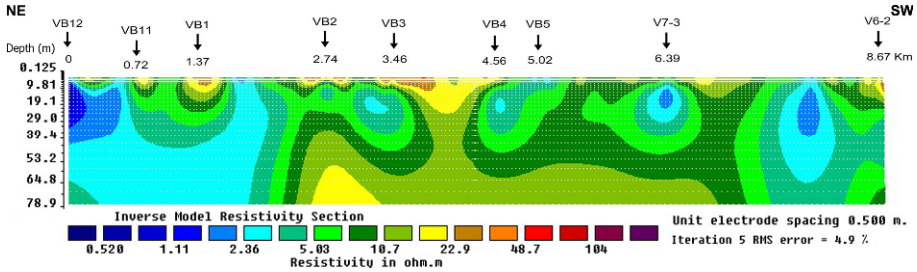

Fig. 8a. The 2D inverted resistivity model along Pr-1 for AB/2 from 3 to 200 m. Colour version of this figure is available in electronic edition only.

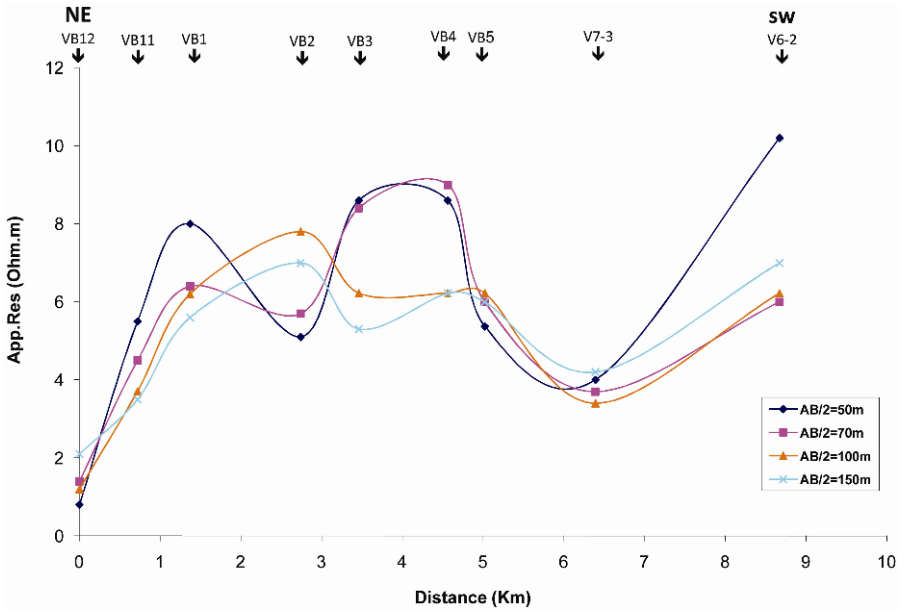

Fig. 8b. Lateral variation of the apparent resistivity along Pr-1 for AB/2 = 50, 70, 100, and 150 m. Colour version of this figure is available in electronic edition only.

shows the lateral variation of the apparent resistivity along Pr–1 for different AB/2 of 50, 70, 100, and 150 m. Pronounced wave-like variation in high and low apparent resistivity can be identifyed along Pr-1 from south to north. Those resistivity variations shown in Fig. 8 reflect the interface between saline and brackich water in the Quaternary deposits in the northern part of the Khanasser valley, where the observed decrease in resistivity is attributed to the intrusion of the saline water.

The established empirical relationship between the interpreted earth resistivity and TDS concentration ($\rho e = -0.0028$ TDS + 15.237) (Asfahani 2007b, 2011) has been applied in order to convert the apparent resistivity

records into estimated TDS values. The estimated TDS values obtained for different AB/2 spacings were used to analyze the TDS variation along the Pr-1 as a function of the AB/2 spacings (Fig. 9). The arrows in Fig. 9 show the salt water propagation, reaching the surface at the VB5 location, where the contact between saline and brackish water is traced. Figure 9 illustrates a supposed movement of saline groundwater from Jaboul salt lake towards the south, as a result of the intensive pumping and a subsequent lowering of the groundwater table. A groundwater flow caused by a hydraulic gradient towards the southern region could not be sustained since there was a groundwater divide in the middle of the valley, between Atshaneh and Rasm Asker, in the first half of May 2002, when pumping was still going on. The salts could actually move towards the hydraulic divide line in the form of a dense saline layer moving southward in the lower Eocene and Quaternary, where the surface of this formation was dipping to the south and the leakage factor of the old lake or periodical transgressions during the wet season permitted the intrusion of salt water (Hoogeveen and Zobisch 1999).

The general trends of the intrusion phenomenon shown in Figs. 8a and 9 have been clarified in greater details through the computation of the layering parameters (resistivities and thicknesses) for the nine VES carried out along Pr-1. This computation has been done by a comparison with a set of master curves (Zohdy *et al*. 1974). The initial model obtained by this comparison is used as starting values in the computer inversion program, in order to get the

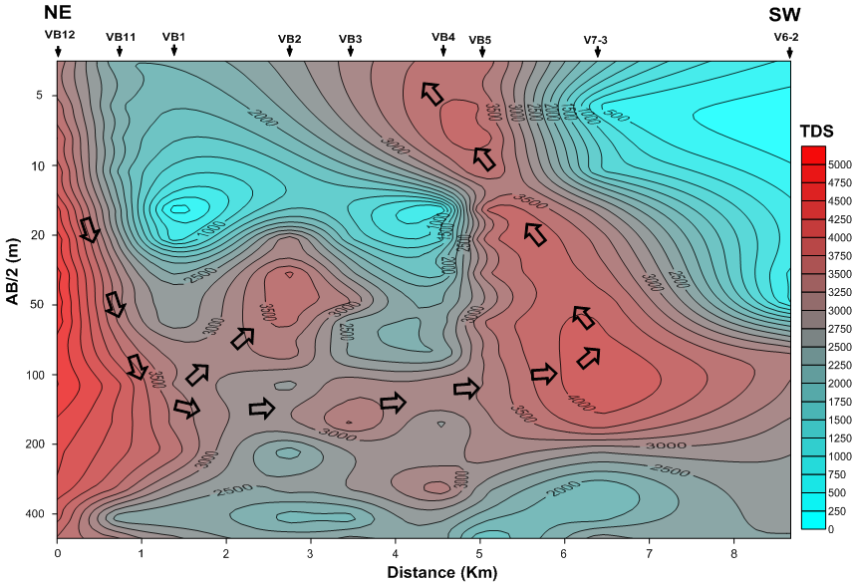

Fig. 9. In-depth variation of TDS along Pr-1 for different AB/2. Colour version of this figure is available in electronic edition only.

best-fit modeled values for each VES, which are shown in Table 2. These modeled resistivity values are thereafter used to construct a geoelectrical section to show the inverted resistivities and depths of the different zones of groundwater quality along Pr-1, as shown in Fig. 10. Three zones of ground-

Table 2

Geoelectrical parameters of the nine studied VES along Pr-1

VES station	No. of layers	Resistivity of layers [Ω·m]					Thickness of layers [m]			
		ρ_1	ρ_2	ρ_3	ρ_4	ρ_5	h_1	h_2	h_3	h_4
VB12	5	5.3	0.6	8.3	3.0	46	6.3	35.7	32.0	120.0
VB11	5	9.3	2.5	6.5	2.5	45	18.8	29.4	27.0	127.5
VB1	5	25.6	6.4	8.9	3.1	45	7.6	18.0	28.0	106.0
VB2	5	89.4	3.7	9.9	4.0	43.6	4.1	20.7	31.6	93.6
VB3	5	75	7.7	5.7	4.6	35	4.0	21.6	30.7	103.0
VB4	5	20.8	9.0	7.1	5.2	30	6.4	22.0	41.3	181.4
VB5	5	4.6	5.2	6.6	6.0	32	4.2	20.7	40.3	151.5
V7-3	3	15.5	3.6	25.5	–	–	6.0	91.0	–	–
V6-2	3	22.6	6.0	15.8	–	–	17.2	199.0	–	–

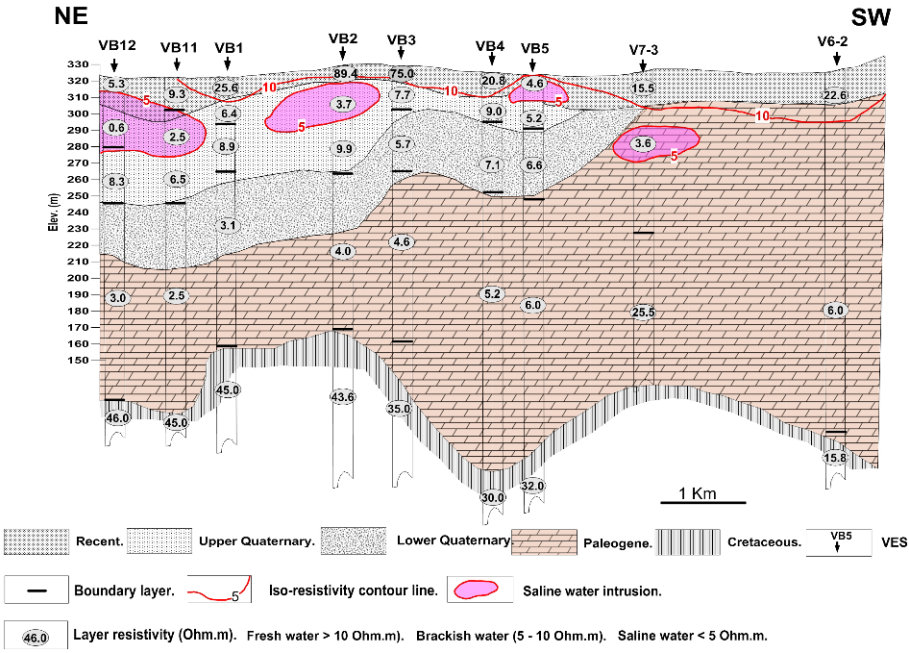

Fig. 10. Geoelectrical section for the different interfaces of water quality along Pr-1. Colour version of this figure is available in electronic edition only.

water quality are depicted through Pr-1. These zones are: fresh water (ρe > 10 Ohm·m), brackish (ρe between 5 and 10 Ohm·m) and saline groundwater (ρe < 5 Ohm·m). The interfaces between those zones of different water quality are well established; the brackish water has a large extension and almost dominates this Pr-1 section. A noticeable low-resistivity anomaly, reaching the surface, is also depicted at the VB5 location, where the well 97 of a depth of 40 m is located. This anomaly may infer a possible saline groundwater up-coning through the Quaternary deposits, although a further characterization should be needed to confirm this phenomenon.

The 1D geoelectrical model for Pr-1 depicted a low-resistivity layer ranging between 2.5 and 6 Ohm·m, interpreted as the Paleogene and Quaternary formations. Such low resistivity records for Quaternary layer infer that it is affected by salt water intrusion with a flow direction towards southeast, and supports the hydrological pattern shown in Fig. 9.

It is to mention that Asfahani (2010, 2011) has previously indicated the hazard of the salt water intrusion in the Khanasser valley while studying the longitudinal LP3 profile, and showed the tendency of the iso-saline TDS contours to be elongated and directed towards the surface, due to the excessive fresh water depletion.

The VES grid used in this paper allowed to derive the hydrological pattern in the northern part of the Khanasser valley and to improve the interpretation of water samples analyzing results of Table 1.

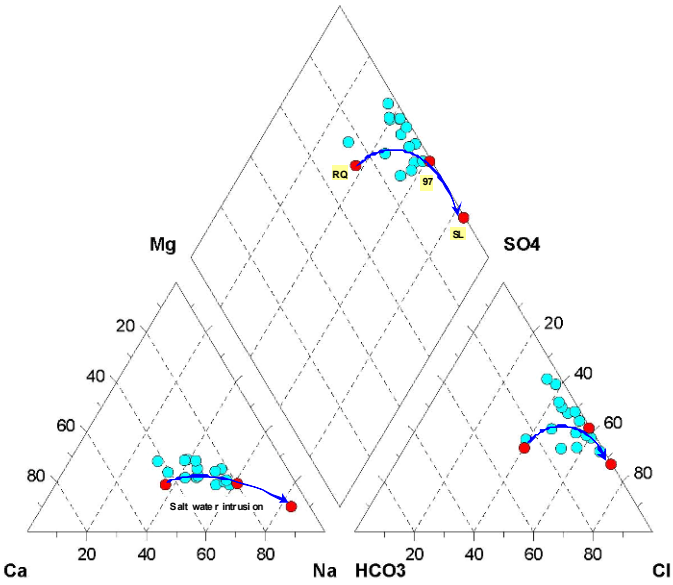

Fig. 11. Piper diagram for shallow groundwater samples. Colour version of this figure is available in electronic edition only.

Three water groups have been obtained through using Piper diagram and mixing ratios (Figs. 11 and 12). The first water group is related to RQ and wells Nos. 115, 202, 233, and 255 located in the slope of Al-Hass and Shbeith mountains (recharge areas) and has calcium bicarbonate composition with a salinity ranging from 300 to less than 2000 mg/l. The second water group is used for irrigation and drinking cattle purposes and has salinity between 2000 to 6000 mg/l (wells Nos. 58, 105, 116, 120, 124, and 239).

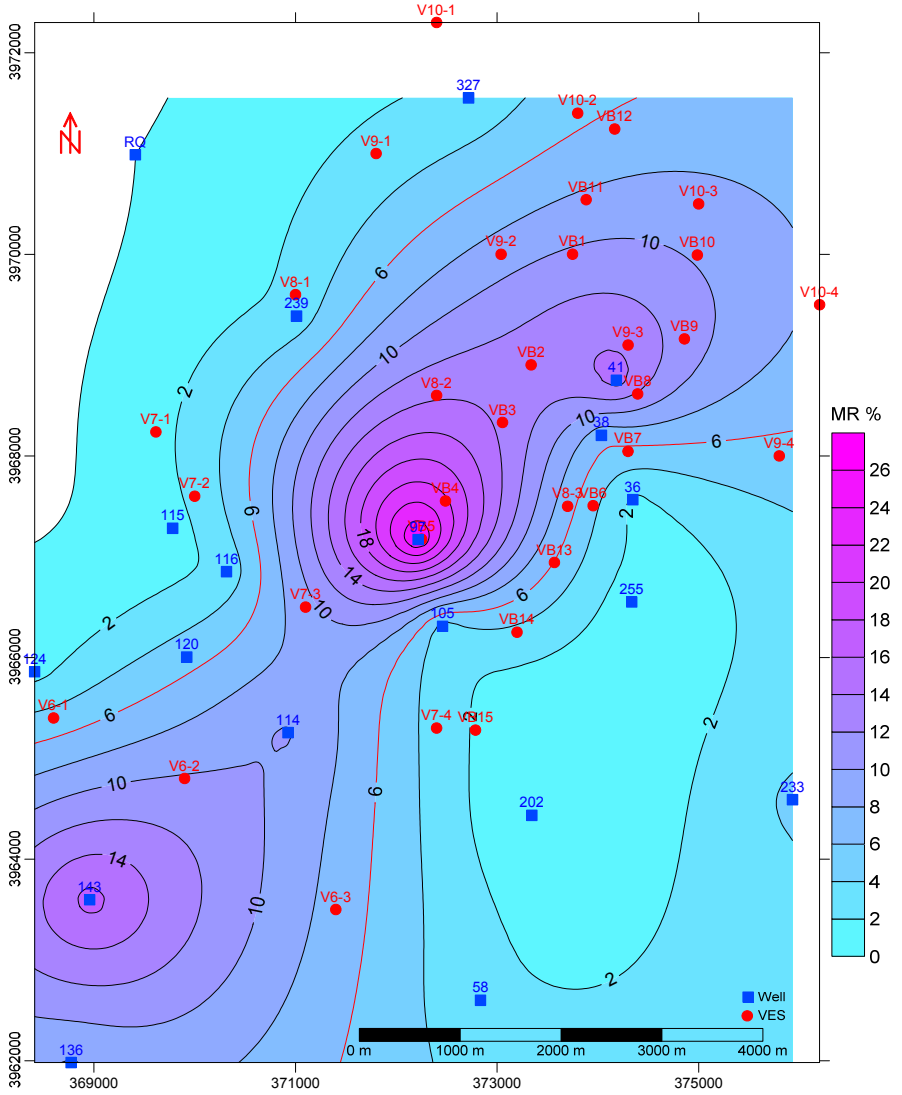

Fig. 12. Mixing ratio (MR%) distribution for shallow groundwater. Colour version of this figure is available in electronic edition only.

The third water group (wells Nos. 38, 41, 97, 114, 136, and 143) has a salinity of more than 5000 mg/l with sodium chloride type. This salinity reaches more than 10000 mg/l in well 97 (Fig. 11), where those wells are out of use due to a putative up-coning salt water intrusion originated from Jaboul salt water lake.

The mixing ratios are estimated by using the chloride masse balance, with the assumption that mixing processes are the major and dominant

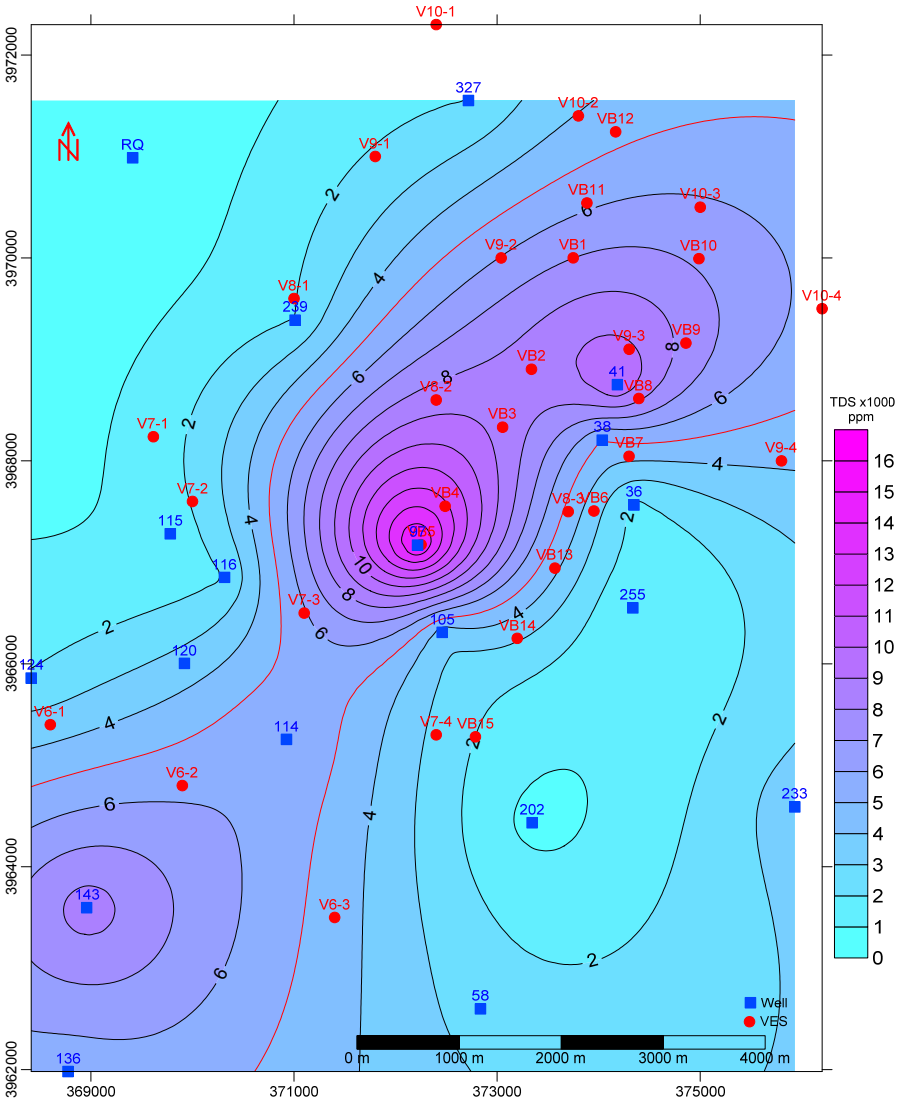

Fig. 13. Distribution map of the measured TDS values of groundwater samples (quaternary aquifer). Colour version of this figure is available in electronic edition only.

mechanism of the groundwater salinization related to the salt water intrusion in the northern part of the Kanasser valley near Jaboul Sabkha.

The mixing ratios of salt water within groundwater are computed by using a reference of fresh water sample, which forms the first end-member. This sample is selected from the old permanent RQ in Shallaleh village, and has a salinity ranging between 0.88 and 0.95 mS/cm during the year. The second end-member is taken from Jaboul Sabkha salt water. The fraction of salt water in the mixing groundwater, MR_S %, is given by the following equation (Herczeg and Edmunds 2000, Abou Zakhem and Hafez 2007):

$$MR_s\% = \left[\left(Cl^-_{GW} - Cl^-_{RQ}\right)\Big/\left(Cl^-_{SL} - Cl^-_{RQ}\right)\right]\times 100 \ ,$$

where MR_s % denotes the fraction of salt water in the mixing groundwater, Cl^-_{GW} the chloride concentration in the mixing groundwater, Cl^-_{RQ} the chloride concentration in the fresh water sample (RQ), first end-member, and Cl^-_{SL} the chloride concentration in the sabkha salt water sample (SL), second end-member.

According to the above equation, a mixing ratios map is established (Fig. 12), where a similar behavior distribution as the electrical resistivity distributions shown in Figs. 4 and 5 is obtained. However, differences between the iso-value maps for mixing ratios (Fig. 12) and the electrical resistivity distribution (Figs. 4 and 5) are partially due to different number and location of data points used to construct these iso-value maps.

The analysis of the mixing ratios shown in Fig. 12 allows clarifying the high influence of the Jaboul Sabkha leakages on the groundwater salinity, particularly in the northern part of the Khanasser valley. The mixing ratio reaches its maximum in well 97 matching with the location of VB5. A mixing ratio of about 6% or higher deteriorates the groundwater quality, consequently becoming out of use. Figure 13 shows the distribution map of the measured TDS values in the analyzed groundwater samples, where similar distribution behavior as the mixing ratios is obtained.

6. CONCLUSIONS

The salt water intrusion in the northern part of the Khanasser valley has been characterized by the joint application approach of both geoelectrical and hydrochemical investigation surveys. The results obtained by those two techniques have been consistent, and similar distributions of resistivity, EC, Cl^-, measured TDS and mixing ratios have been obtained. However the apparent differences between the distributions of geoelectrical resistivity, EC, and mixing ratios are related to the limited number of the observatory wells in the Khanasser valley. This proves the importance of using the geoelectrical methods as a useful guide in a coherent combination with the

hydrochemical investigation for characterizing the salt water intrusion and determining the interfaces between different water qualities. Moreover, the hydrochemical investigations carried out in this research confirm the consistency of different geoelectrical methods in solving hydrogeological problems, such as the salt water intrusion. By means of geoelectrical surveying the different salt water intrusion trends have been laterally and vertically established.

A putative salt-water up-coning was also identified at the location of VB5 and well 97. Likely in response to intense fresh water pumping, the fresh-water/salt-water interface moved vertically toward the pumping well 97 head. The wells severely salinized, as the well 97, are actually out of use due to the excessive fresh-water depletion which affects the quality of groundwater by upward of deep flow of saline water, as shown along Pr-1, and this should be avoided. Therefore, it is important to monitor and keep the fresh-salt water interface in a stationary situation by pumping a limited amount of groundwater, based on the available fresh water and the water balance in the region.

Acknowledgments. Authors would like to thank Dr. I. Othman, General Director of Syrian Atomic Energy Commission (SAEC) for permition to publish this paper.

The German Ministry of Economic Cooperation and Development (BMZ) and German Agency for Technical Cooperation (GTZ) are acknowledged for financial and administrative support to the Khanasser Valley Integrated Research Site (KVIRS) project. Professor Rieser Armins (coordinator of the project) from Bonn University, Germany, is deeply thanked for many useful discussions during the preparation stages of this project.

ICARDA is highly thanked for providing all the facilities during the Khanasser project.

The anonymous reviewers are cordially thanked for their professional suggestions and remarks. Dr. Majid Beiki, associate editor of *Acta Geophysica*, is deeply thanked for his critical suggestions and remarks that considerably improve the final revised version.

References

Abou Zakhem, B., and R. Hafez (2007), Environmental isotope study of seawater intrusion in the coastal aquifer (Syria), *Environ. Geol*. **51**, 8, 1329-1339, DOI: 10.1007/s00254-006-0431-x.

ACSAD (1984), Water resources map of the Arab countries, The Arab Center for the Studies of Arid Zones and Dry Lands, Damascus, Syria.

Al-Sayed, E.A., and G. El-Qady (2007), Evaluation of sea water intrusion using the electrical resistivity and transient electromagnetic survey: Case study at Fan of Wadi Feiran, Sinai, Egypt. **In:** *EMG 2007 International Workshop "Innovation in EM, Grav and Mag Methods: A New Perspective for Exploration", 15-18 April 2007, Capri, Italy.*

Asfahani, J. (2007a), Geoelectrical investigation for characterizing the hydrogeological conditions in semi-arid region in Khanasser valley, Syria, *J. Arid Environ*. **68**, 1, 31-52, DOI: 10.1016/j.jaridenv.2006.03.028.

Asfahani, J. (2007b), Electrical earth resistivity surveying for delineating the characteristics of ground water in a semi-arid region in Khanasser valley, northern Syria, *Hydrol. Process*. **21**, 8, 1085-1097, DOI: 10.1002/hyp.6290.

Asfahani, J. (2007c), Neogene aquifer properties specified through the interpretation of electrical sounding data, Salamiyeh region, central Syria, *Hydrol. Process*. **21**, 21, 2934-2943, DOI: 10.1002/hyp.6510.

Asfahani, J. (2010), Application of surfacial geoelectrical resistivity technique in hydrogeology domain for characterizing saline groundwater in semi arid regions. **In:** B. Veress and J. Szigethy (eds.), *Horizons in Earth Science Research*, Vol. 1, NOVA Science Publishers, New York, 351-381.

Asfahani, J. (2011), Electrical resistivity investigations for guiding and controlling fresh water well drilling in semi-arid region in Khanasser valley, northern Syria, *Acta Geophys.* **59**, 1, 139-154, DOI: 10.2478/s11600-010-0031-8.

Asfahani, J. (2012a), Quaternary aquifer transmisivity derived from vertical electrical sounding measurements in the semi-arid Khanasser valley region, Syria, *Acta Geophys*. **60**, 4, 1143-1158, DOI: 10.2478/s11600-012-0016-x.

Asfahani, J. (2012b), Groundwater potential estimation deduced from vertical electrical sounding measurements in the semi-arid Khanasser valley region, Syria, *Hydrol. Sci. J*. (in print).

Asfahani, J., and Y. Radwan (2007), Tectonic evolution and hydrogeological characteristics of Khanasser valley, northern Syria, derived from the interpretation of vertical electrical soundings, *Pure Appl. Geophys*. **164**, 11, 2291-2311, DOI: 10.1007/s00024-007-0274-8.

Ayers, J.F. (1989), Conjunctive use of geophysical and geological data in the study of an alluvial aquifer, *Ground Water* **27**, 5, 625-632, DOI: 10.1111/j.1745-6584.1989.tb00475.x.

Herczeg, A.L., and W.M. Edmunds (2000), Inorganic ions as tracers. **In:** P.G. Cook and A.L. Herczeg (eds.), *Environmental Tracers in Subsurface Hydrology*, Kluwer Academic Publ., Dordrecht, 31-78.

Hoekstra, P. (1990), Surface geophysics – Tool for ground water management in coastal aquifers, *Water Wastewater Int*. **5**, 3, 15-21.

Hoogeveen, R., and M. Zoebisch (1999), Decline of groundwater quality in Khanasser valley (Syria) due to salt water intrusion. **In:** *6th Int. Conf. on the Development of Dry Lands, 22-27 August 1999, Cairo, Egypt*, 16 pp.

Hussein, M.T., and H.S. Awad (2006), Delineation of groundwater zones using lithology and electric tomography in the Khartoum basin, central Sudan, *Comp. Rend. Geosci.* **338**, 16, 1213-1218, DOI: 10.1016/j.crte.2006.09.007.

Loke, M.H. (1996), The use of electrical imaging surveys for mapping subsurface pollution. **In:** *Prosiding Seminar Geologi & Sekitaran: Impak dan Pengauditan, Bangi*, 223-232.

Nassir, S.S.A., and C.Y. Lee (1998), The use of geoelectrical surveys for the delineation of different subsurface geological and man-made features. **In:** *Ninth Regional Congress on Geology, Mineral and Energy Resources of Southeast Asia, Kuala Lumpur*, 70-71.

Pichgin, N.I., and I.K.H. Habibullaev (1985), Methodological recomendations in studying geo-tectonic conditions of vertical electrical soundings data with application of EC computer for solving hydrogeological and geo-engineering problems, Tashkend (in Russian).

Ponikarov, V.P. (1964), The geological map of Syria, 1:200.000 and explanatory notes, Ministry of Industry, Department of Geological and Mineral Research, Damascus, Syria.

Reilly, T.E., and A.S. Goodman (1985), Quantitative analysis of saltwater-freshwater relationships in groundwater systems – A historical perspective, *J. Hydrol*. **80**, 1-2, 125-160, DOI: 10.1016/0022-1694(85)90078-2.

Samsudin, A.R., A. Haryono, U. Hamzah, and A.G. Rafek (1997), Salinity study of coastal groundwater aquifers in North Kelantan, Malaysia, *Bull. Geol. Soc. Malaysia* **41**, 59-165.

Soumi, G. (1991), Supplemental irrigation systems of the Syrian Arab Republic (SAR). **In:** *Proc. Workshop on Regional Consultation on Supplemental Irrigation, ICARDA and FAO, 7-9 December 1987, Rabat, Morocco*, Kluwer Academic Publishers, Dordrecht, 497-511.

Todd, D.K. (1980), *Ground Water Hydrology*, 2nd ed., John Wiley and Sons, New York, 535 pp.

Zohdy, A.A.R., G.P. Eaton, and D.R. Mabey (1974), Application of surface geophysics to ground-water investigations, Techniques of Water-Resource Investigation, U.S. Geol. Surv.

Received 24 November 2011
Received in revised form 11 June 2012
Accepted 3 July 2012